Machine Vision and Applications (2000) 11: 257–263

Machine Vision and Applications


# Machine tool condition monitoring using workpiece surface texture analysis

**Ashraf A. Kassim**[1], **M.A. Mannan**[2], **Ma Jing**[1]

[1] Department of Electrical Engineering, National University of Singapore, 10 Kent Ridge Crescent, Singapore 119260
[2] Department of Mechanical and Production Engineering, National University of Singapore, 10 Kent Ridge Crescent, Singapore 119260

Received: 9 June 1998 / Accepted: 6 October 1999

**Abstract.** Tool wear affects the surface roughness dramatically. There is a very close correspondence between the geometrical features imposed on the tool by wear and micro-fracture and the geometry imparted by the tool on to the workpiece surface. Since a machined surface is the negative replica of the shape of the cutting tool, and reflects the volumetric changes in cutting-edge shape, it is more suitable to analyze the machined surface than look at a certain portion of the cutting tool. This paper discusses our work that analyzes images of workpiece surfaces that have been subjected to machining operations and investigates the correlation between tool wear and quantities characterizing machined surfaces. Our results clearly indicate that tool condition monitoring (the distinction between a sharp, semi-dull, or a dull tool) can be successfully accomplished by analyzing surface image data.

**Key words:** Tool condition monitoring – Surface texture analysis – Image processing – Computer Vision

## 1 Introduction

Tool wear affects the surface morphology dramatically. The shape of a cutting tool changes due to different types of wear on the tip, flank and rake. There is a very close correspondence between the geometrical features imposed on the tool by wear and micro-fracture, and the geometry imparted by the tool onto the workpiece surface. A machined surface carries valuable information about the process, including tool wear, built-up edge and vibrations. Under the stable machining conditions the surface texture changes remarkably due to the changes in cutting tool shape caused by wear. Since the cutting tool operates directly on the workpiece, it affects the texture of the workpiece surface, which in turn provides reliable and detectable information to categorize the condition of the cutting tool.

Many researchers have investigated the correlation between the surface roughness and texture and tool condition in finishing, diamond-turning and grinding operations. In [12], [13] and [14], random process analysis techniques, including spectral analysis of the surface waviness were applied to characterize the surfaces generated by sharp and dull tools. In [6] and [8], the autocorrelation technique was applied to characterize the machined surfaces. Several others have developed optical systems to measure the tool flank wear and crater wear in turning [2, 3, 10].

A machined surface is the negative replica of the shape of the cutting tool, and it reflects the volumetric changes in the shape of the cutting edge. Also, it is easier to analyze the machined surface than to look at certain portions of the cutting tool, which is normally the case with the optical systems for flank wear measurement. Although some systems have more complex optical heads to look at both the flank and crater wear, they still provide incomplete information. Furthermore, these optical systems are more complex and costly. Our texture analysis system uses a CCD camera with a high-magnification lens. This system provides sufficient information about a machined surface and is much faster than a stylus-based system. There are many texture discrimination methods [7, 9, 11]. However, real-world textures are often not uniform, due to changes in orientation, scale or other visual appearances. Furthermore, texture discrimination methods are usually computationally intensive. In this paper, images of the workpiece surfaces are analyzed to distinguish sharp tools from dull ones using machine vision techniques.

## 2 Experimental investigation

### *2.1 Experimental set-up*

In our experiments, we turned different AISI 1045 and AISI 4340 workpiece materials with different grades and makes of coated and uncoated cemented carbide inserts for different machining periods. The turning operation lasted until the inserts reached catastrophic failure. After each pass, the surfaces of the resulting machined workpieces were imaged as 640 × 480-pixel *grey-level* digital images using a CCD camera (with a high-magnification lens) connected to a computer equipped with image acquisition capability. The corre-

*Correspondence to*: (e-mail: ashraf@nus.edu.sg)

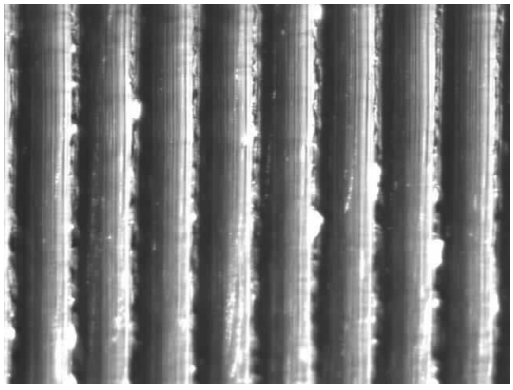

**a**

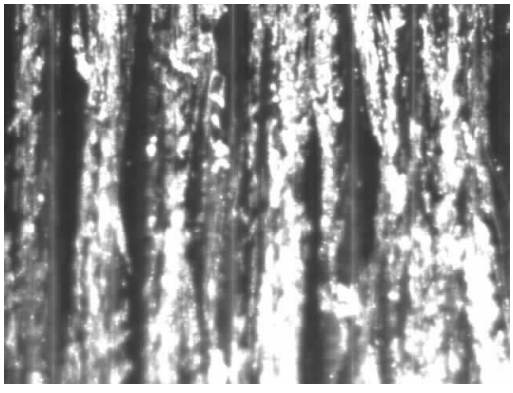

**b**

**Fig. 1. a** Surface machined by a sharp tool and **b** surface machined by a dull tool

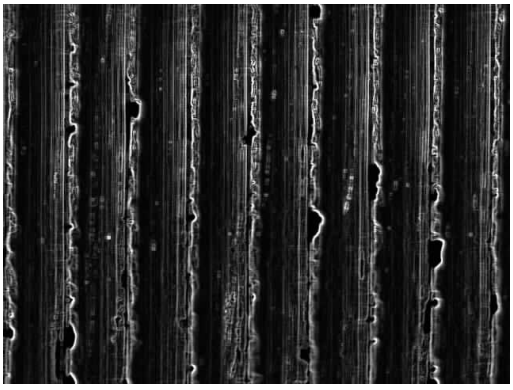

**a**

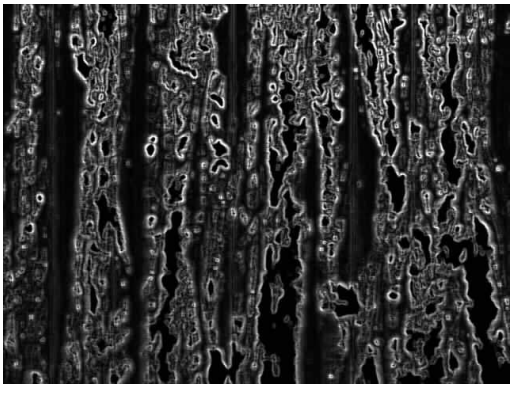

**b**

**Fig. 2a,b.** Gradient images of **a** Fig. 1a and **b** Fig. 1b

sponding flank wear of the cutting tool was also measured. A large number of roughing (dry turning) tests have been conducted using different combinations of cutting speeds (100–300 m/min) and feeds (0.3–0.8 mm/rev). In all tests, the depth of cut was kept at 3 mm. The results reported in Sect. 4, are from the machining tests with two different sets of cutting data and workpiece materials. In set A, AISI 1045 workpieces were turned at the feed rate of 0.4 mm/rev and the cutting speed of 220 m/min. In set B, the cutting speed was selected at 120 m/min to turn AISI 4340 workpieces with feed rate of 0.3 mm/rev.

### *2.2 Image capture*

Figure 1 shows the digital images of surfaces machined with a sharp insert and a dull insert from one of the tests. A CCD camera is placed at a certain distance over the workpiece and the images of turned surfaces are captured at certain predefined positions. The images of each set are ordered by assigning an image number according to the level of wear of the insert. The higher the image number, the greater the level of wear of the insert, and therefore the poorer the quality of the machined surface.

## 3 Image-processing techniques for surface texture analysis

The grooves evident in the images are formed by the insert during machining. The texture within each groove is determined by the manner in which the metal is machined. Generally, as the insert becomes blunt, wear particles on the machined surface become more apparent and the texture of the machined surface becomes more irregular. Image *segmentation* techniques [5] and *texture analysis* methods [1] can be used to bring out the differences between the images. Image segmentation involves dividing an image into areas that have some physical significance and therefore represents spatial analysis of the regions of interest in the image. The segmentation process first involves extraction of edge information from the images using the *Sobel operator* [4], and this is followed by a *thresholding* [4] operation. After the Sobel operation, the wear particles become more apparent in the resulting *gradient image*, as illustrated in Fig. 2, and are easily visible in the resulting *binary images* after thresholding, as illustrated in Fig. 3. The thresholds were obtained by simple analysis of histograms of the respective gradient images. The following sub-sections describe two techniques that use the processed digital images to distinguish between surfaces machined with a sharp tool and those machined with a dull tool.

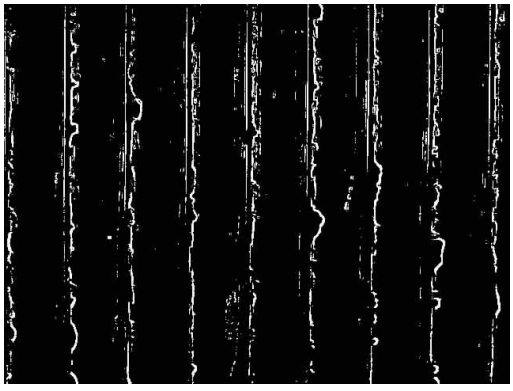

**a**

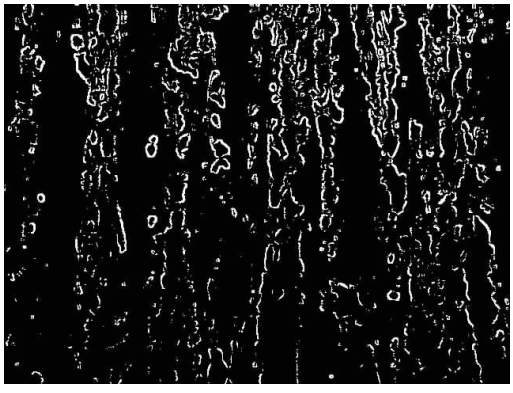

**b**

**Fig. 3a,b.** Binary images of the machined surfaces of the set A material for **a** surface machined by a sharp tool and **b** surface machined by a dull tool

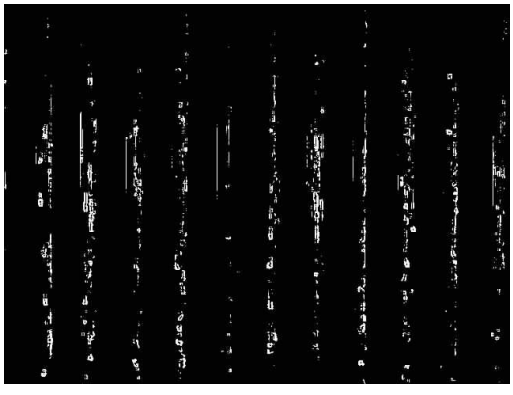

**a**

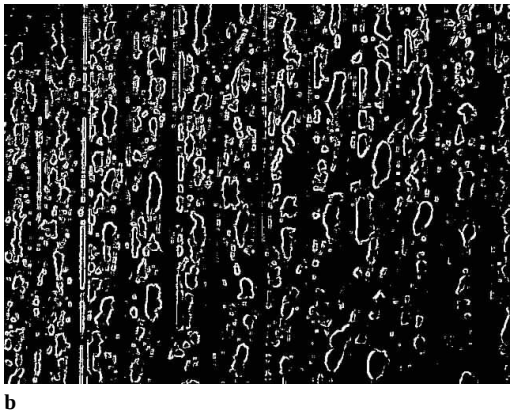

**b**

**Fig. 4a,b.** Binary images of the machined surface of the set B material for **a** surface machined by a sharp tool and **b** surface machined by a dull tool

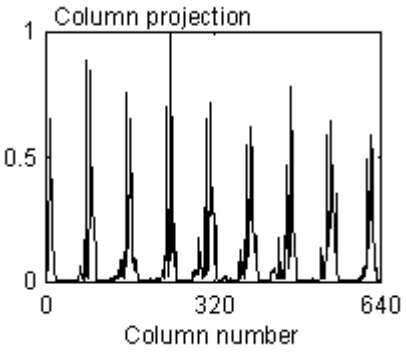


**a**

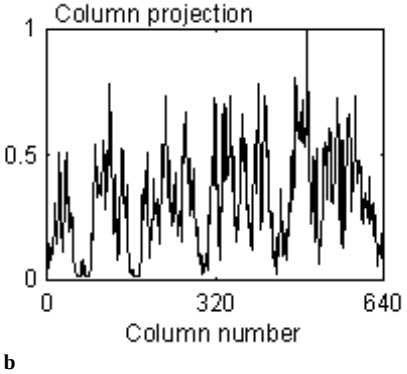


**b**

**Fig. 5a,b.** Column projections of the **a** image of Fig. 3a, and **b** image of Fig. 3b

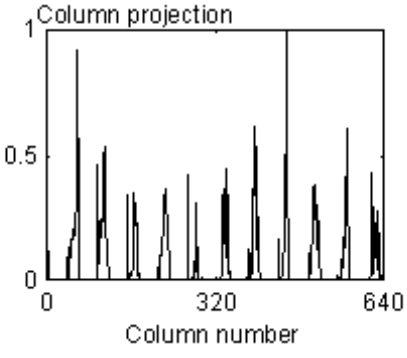


**a**

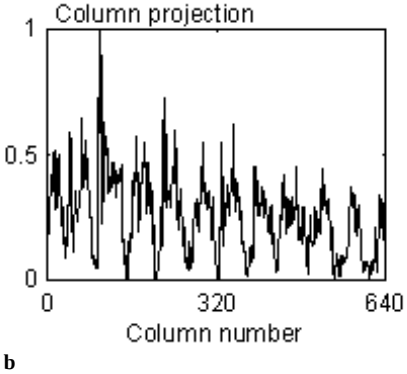


**b**

**Fig. 6a,b.** Column projections of the **a** image of Fig. 4a, and **b** image of Fig. 4b

| | | | | |
|---|---|---|---|---|
| 1 | 2 | 3 | 2 | 1 |
| 1 | 2 | 1 | 3 | 1 |
| 2 | 3 | 2 | 1 | 2 |
| 3 | 1 | 2 | 1 | 2 |
| 3 | 1 | 3 | 2 | 3 |

Image *A*

| $I$ \ $j$ | **1** | **2** |
|---|---|---|
| **1** | 1 | 4 |
| **2** | 3 | 3 |
| **3** | 5 | 1 |

Run length matrix *P*

**Fig. 7.** Run-length matrix $P$ generated from image $A$

### *3.1 Column projection analysis*

This technique operates on the *thresholded gradient images* (i.e., binary images; Fig.4) of the machined surfaces. *Column projections* are obtained by adding all pixel values along each column of the processed image data, thereby reducing the 2D binary image to a 1D array that can be processed quickly. The 1D column projection array, illustrated in Figs. 5 and 6, is normalized with respect to the largest peak to eliminate the non-uniformity of the sources of illumination. It is apparent from Figs. 5 and 6 that the peaks obtained from the column projections of the surfaces machined with a sharp tool are quite distinct from those obtained from the surfaces machined with a dull tool. The area under the peaks can be used to distinguish surfaces machined with a sharp tool from surfaces machined with a dull tool. In Fig. 5a and b, the equidistant peaks correspond to the feed marks. The grooves produced by the feed motion of the cutter are predominant in the actual turned surfaces. As the cutting edge becomes more irregular with scars at the cutting tip, the appearance of the machined surface tends to be more smeared and the grooves corresponding to the feed marks become less predominant. Figures 5b and 6b clearly illustrate this well-known phenomenon.

### *3.2 Run-length statistical method*

*Run-length statistical methods* [1] operate directly on the gradient images (without thresholding). Before the application of these methods, a 2D matrix called the *run-length matrix* $P$ is computed. The elements $p(i, j)$ of the run-length matrix $P$ represent the number of grey-level runs of length $j$ and grey level $i$. Consecutive pixels of the same grey value or level in either the horizontal or vertical direction constitute a run. In this paper, the run-length matrix $P$ is obtained in the vertical direction. As an example, the run-length matrix $P$ in vertical direction of image $A$ is as illustrated in Fig. 7.

The run-length statistics used in this paper are defined by the following equations and are *short-run emphasis* (SRE), *long-run emphasis* (LRE), *run-length nonuniformity* (RLN), *run percentage* (RP), *low-grey-level-run emphasis* (LGRE) and *high-grey-level-run-length emphasis* (HGRE).

$$RNL = \frac{1}{s}\sum_{j=1}^{N}\left(\sum_{i=1}^{M} p(i,j)\right)^2; \tag{1}$$

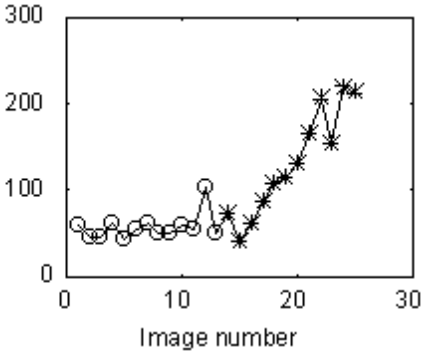


**a**

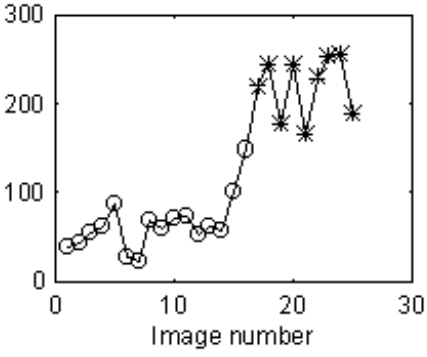


**b**

**Fig. 8a,b.** Area under the column projection peaks vs. image number for **a** set A, and **b** set B

$$RP = \frac{1}{n}\sum_{i=1}^{M}\sum_{j=1}^{N} p(i,j); \tag{2}$$

$$SRE = \sum_{i=1}^{M}\sum_{j=1}^{N}\frac{p(i,j)}{j^2}; \tag{3}$$

$$LRE = \frac{1}{s}\sum_{i=1}^{M}\sum_{j=1}^{N} j^2 p(i,j); \tag{4}$$

$$LGRE = \sum_{i=1}^{M}\sum_{j=1}^{N}\frac{(p(i,j)/s)}{j^2}; \tag{5}$$

$$HGRE = \frac{1}{s}\sum_{i=1}^{M}\sum_{j=1}^{N} i^2 p(i,j). \tag{6}$$

In the above equations, $M$ is the number of grey-levels, $N$ is the longest run, $s$ is the total number of runs in the image, and $n$ is the number of pixels in the image. The next section discusses the results obtained by applying these techniques to the images of the machined surfaces.

## 4 Results and observations

Figure 8 shows the area under the peaks of the column projection data for all images in each set. The plots clearly show that the area increases as the quality of the machined surface deteriorates.

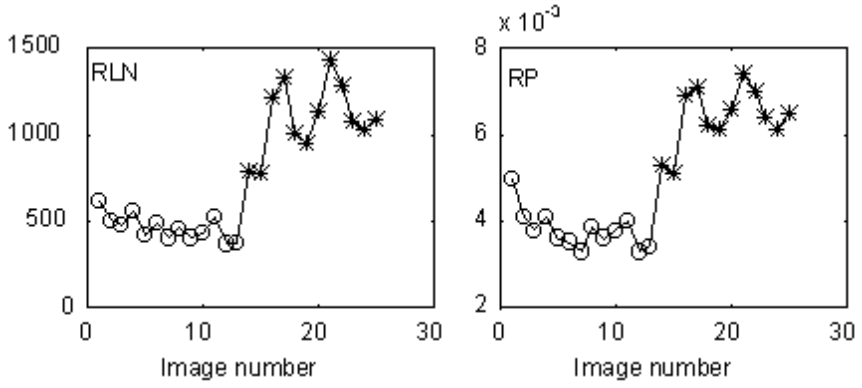


a

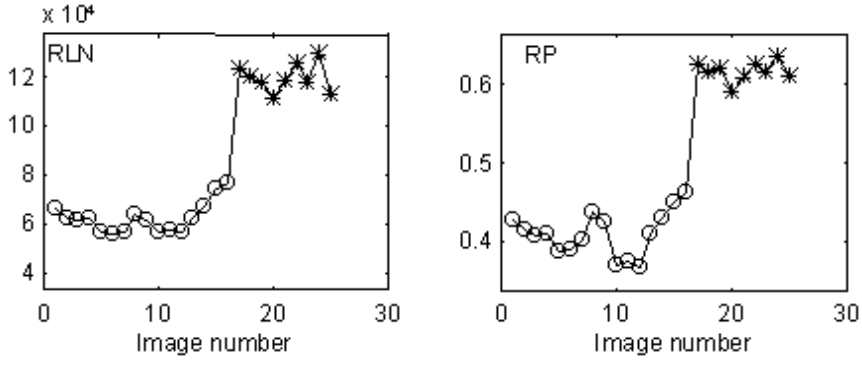


b

**Fig. 9a,b.** Run-length statistical parameters RLN and RP versus image number for **a** set A, and **b** set B

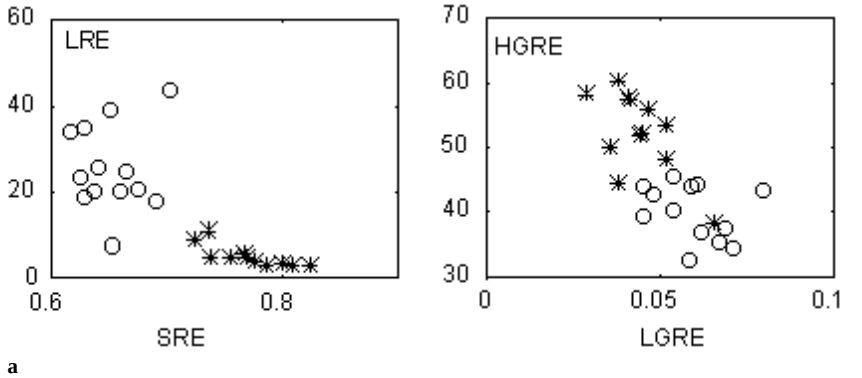


a

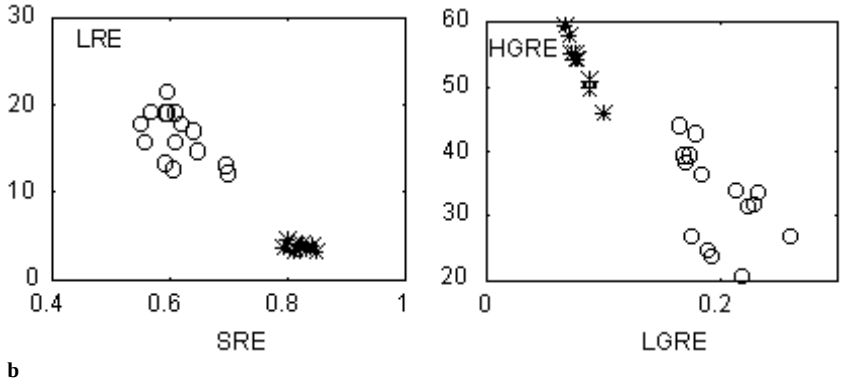


b

**Fig. 10a,b.** Run-length statistical parameters LGE vs. SRE and HGRE vs. LGRE for **a** set A and **b** set B

From Fig. 9, it is evident that the RLN and the RP parameters increase as the quality of the machined surface deteriorates. This is expected, since the non-uniformity of the vertical image pixels increases as the image surface deteriorates. When the other run-length statistical parameters are also plotted against the image numbers, it becomes evident that they do not provide as good an indication of the deterioration of the machined surface as that provided by RLN

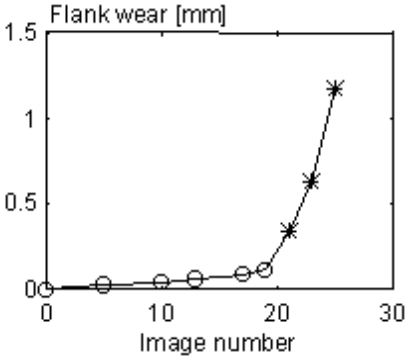


**a**

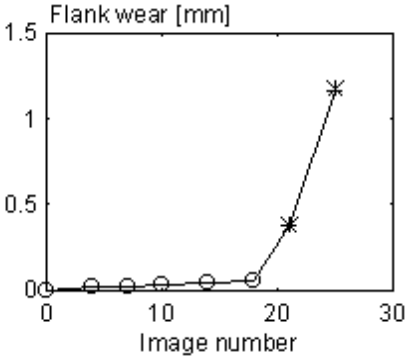


**b**

**Fig. 11a,b.** Tool wear vs. image number for **a** set A and **b** set B

and RP. However, good discrimination between surfaces machined with a sharp tool and surfaces machined with a dull tool is provided by the LRE versus SRE plots, and HGRE versus LGRE plots as shown in Fig. 10.

From Figs. 8, 9 and 10, we also find that the ability to distinguish between different surfaces generated by sharp and dull tools, is better for set B than the set A. A possible reason for this may be the different workpiece material used in set B. Generally, the wear pattern on a cutting edge is more uniform, consistent and repeatable while machining a harder and tougher high-alloyed tool steel as compared to the wear pattern induced by turning of low- and medium-carbon steels.

Figure 11 shows the corresponding flank wear of the tool as the quality of the machined surfaces deteriorates as measured by an optical microscope. It is very clear that the processed information from the digital images of the machined surfaces clearly point to increased deterioration and therefore increased probability of tool breakage even before it happens, as is indicated by the flank wear information. This very significant result implies that machine vision techniques are excellent for monitoring cutting-tool condition in roughing (dry cutting) and will be helpful to prevent damage to the machine tool.

## 5 Concluding remarks

Processing the column projection data by monitoring the area under the peaks and calculating the run-length statistical parameters are effective in directly monitoring the deterioration of machined surfaces, and therefore indirectly monitoring the condition of the cutting tool.

Using a Pentium 166-MHz computer with image acquisition capability, the whole monitoring procedure including image capture and image analysis can be performed in seconds. The column projection method took under 8 s, while the run-length statistical method took under 20 s. Typical tool life of a turning tool is several minutes, and so the techniques presented in this paper can be used for offline tool condition monitoring in real production environments.

It is evident from the results presented in Figs. 6 and 8 that the run-length statistical method provides better discrimination between a sharp and a dull tool as compared with that provided by the column projection method. Both of our image analysis methods (see Figs. 6 and 8) provide earlier detection of the onset of catastrophic failure as compared with the conventional flank wear measurements (see Fig. 10). From Figs. 6, 8 and 9, we also find that the ability to distinguish between surfaces machined wit h a sharp tool from surfaces machined with a dull tool is better for set B than for set A. A possible reason for this is that the material used in Set B is prehardened and tempered high-tensile Nickel Chromium steel (AISI4340).

We have shown that machine vision techniques can be applied to effectively monitor the condition of the cutting tool (a sharp, semi-dull, or a dull tool) by analyzing the machined surfaces. The encouraging results of our work paves the way for the development of a real-time, low-cost, and reliable tool-condition-monitoring system.

*Acknowledgements.* The authors would like to thank Ms HS Seow for her contributions to this work. The authors would also like to thank Mr Sukiantor of Workshop 2, Mechanical Engineering Department, National University of Singapore.

## References

1. Chu A, Sehgal CM, Greenleaf JF (1990) Use of grey-value distribution of run lengths for texture analysis. Pattern Recognition Lett 11:415–420
2. Byrne G, Dornfeld D, Inasaki I, Ketteler G, Koning W, Teti R (1995) Tool Condition Monitoring (TCM) – The status of research and industrial applications. Ann CIRP 44(2): 541–568
3. Giutsi F, Santoschi (1984) A flexible tool wear sensor for NC lathes. Ann CIRP 33(1): 229–232
4. Jain AK (1989) Fundamentals of Digital Image processing. Prentice Hall, New York
5. Jain R, Kasturi R, Schunck BG (1995) Machine Vision. McGraw-Hill, New York
6. Kubo M, Peklenik J (1968) An analysis of microgeometric isotropy of random surface structure. Ann CIRP 17: 235–238
7. Goldstein MD, Nagler M (1987) Real time inspection of a large set of surface defects in metal parts. (Automated Inspection and High Speed Vision Architecture) Proc. of the SPIE, Vol 849, pp 184–186
8. Peklenik J (1963) Contribution to the theory of surface characterisation. Ann CIRP 12: 173–178
9. Sharma DK, Rao BV (1993) Machined surface texture parameters for occluded scene segmentation. Proc SPIE, Vol 2183, pp 182–192
10. Spirgeon D, Slater AC (1974) In-process indication of surface roughness using a fiber optics transducer. Proc. of 15th Int. Machine Tool Design and Research Conf. 1974, pp 339–347
11. Teshima T, Shibasaka T, Takama M, Yamamoto A, Iwata K (1993) Estimation of cutting tool life by processing tool image data with neural network. Ann CIRP 42(1): 59–62

12. Whitehouse DJ (1971) Typology of manufactured surfaces. Ann CIRP 18: 417–420
13. Whitehouse DJ (1974) Assessment of surface typology analysis techniques in turning. Ann CIRP 23(2): 265–274
14. Whitehouse D J (1978) Surfaces – A link between manufacture and function. Proc Inst Mech Eng 192: 178–188

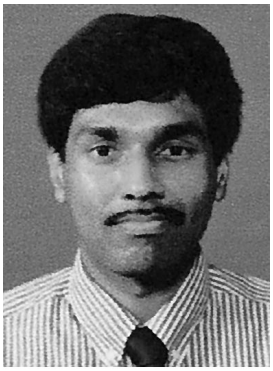

**Ashraf A. Kassim** received his B.Eng. (Hons) and M.Eng. degrees in Electrical Engineering from the National University of Singapore in 1985 and 1987, respectively. Dr. Kassim worked on the design and development of machine vision systems at Texas Instruments for some years before going on to obtain his Ph.D. degree in Electrical and Computer Engineering from Carnegie Mellon University, Pittsburgh, in 1993. Since 1993, he has been with the Electrical Engineering Department at the National University of Singapore, where he is currently an Associate Professor. Dr. Kassim's research interests include multi-processor systems, neural networks, robot guidance, machine vision, and image processing.

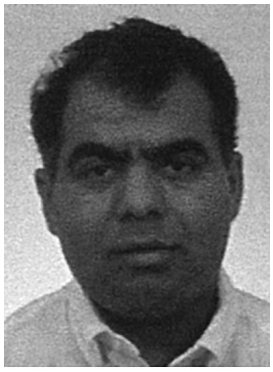

**M. A. Mannan** obtained his M.Sc (Hons) in Machine Tools and Manufacturing Engineering in 1975 from PFU, Moscow on a Government of India scholarship. He joined the Royal Institute of Technology (KTH) in 1975 and was affiliated with the same until 1994, where he held different positions, including research engineer, research associate, research scientist and associate professor. In 1987, the academic title of Docent was conferred on him by KTH. Dr. Mannan joined NUS in 1994 as a senior visiting fellow and is now an Associate Professor with the Mechanical and Production Engineering Department. Dr. Mannan is a corresponding member of the CIRP and a member of ASME.

**Ma Jing** received her B.Eng and M.Eng from the College of Marine Engineering, Northwesterm Polytechnical University, People's Republic of China. She has been a graduate student with the Electrical Engineering Department at the National University of Singapore since 1997. Her research interests include machine vision, image and signal processing, artificial intelligence, and neural networks.